

# Lawrence Berkeley National Laboratory

## LBL Publications

### Title

Achieving diffraction-limited performance on the Berkeley MET5

### Permalink

<https://escholarship.org/uc/item/7xf352nz>

### ISBN

9781510625617

### Authors

Miyakawa, Ryan  
Anderson, Chris  
Zhu, Wenhua  
[et al.](#)

### Publication Date

2019-03-26

### DOI

10.1117/12.2516384

Peer reviewed

# Achieving Diffraction-limited Performance on the Berkeley MET5

Ryan Miyakawa\*, Chris Anderson, Wenhua Zhu, Geoff Gaines, Jeff Gamsby, Carl Cork, Gideon Jones, Michael Dickenson, Seno Rekawa, Weilun Chao, Sharon Oh, and Patrick Naulleau  
Center for X-ray Optics, Lawrence Berkeley National Lab, 1 Cyclotron Road, Berkeley, CA USA  
94720

## ABSTRACT

The Berkeley MET5, funded by EUREKA, is a 0.5-NA EUV projection lithography tool located at the Advanced Light Source at Berkeley National Lab. Wavefront measurements of the MET5 optic have been performed using a custom in-situ lateral shearing interferometer suitable for high-NA interferometry. In this paper, we report on the most recent characterization of the MET5 optic demonstrating an RMS wavefront 0.31 nm, and discuss the specialized mask patterns, gratings, and illumination geometries that were employed to accommodate the many challenges associated with high-NA EUV interferometry.

## 1. INTRODUCTION

As the next generation of EUV lithography tools moves toward high numerical apertures ( $NA > 0.5$ ), it is becoming increasingly important to characterize and remove optical aberrations to achieve performance near the diffraction limit. At the same time, measuring wavefronts at high NA presents numerous additional challenges [1]. Existing interferometric solutions are complicated by the difficulty of finding a bright, high quality reference wave, and by nonlinear effects associated with high incident angles on interferometry targets [2]. The interferometry program on the Berkeley MET5 has overcome these obstacles by designing and implementing a lateral shearing interferometer that uses specialized mask and image-plane grating targets as well as a novel reconstruction procedure. This design allows the interferometer to accurately measure aberrations in the tool despite its large NA and non-telecentric geometry. In this paper, we present various design considerations of the MET5 interferometry module and report on the latest measurements following the optical alignment of the tool demonstrating an RMS wavefront of 0.31 nm.

## 2. IN-SITU LATERAL SHEARING INTERFEROMETER MODULE

### 2.1 Module integration

The lateral shearing interferometry (LSI) module sits directly adjacent to the print module on the MET5 imaging subsystem. A schematic of this subsystem is shown in Figure 1.

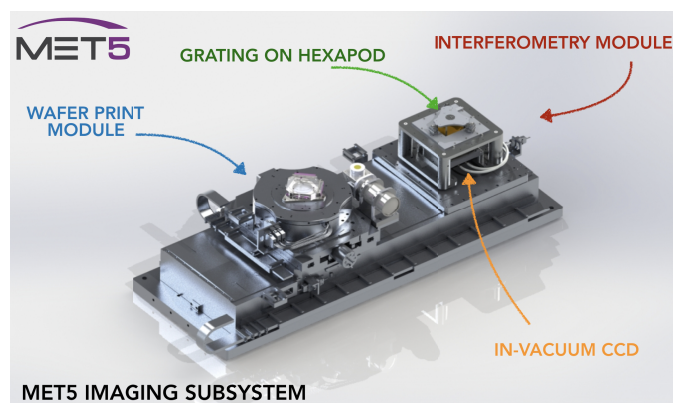


Figure 1. The MET5 imaging subsystem showing the wafer print module adjacent to the interferometry module.

\*rhmiyakawa@lbl.gov

Both modules are mounted to a long-range linear stage which allows the MET5 to easily switch between printing and interferometry modes. This design allows for the periodic monitoring of the tool alignment over time to ensure that the optic is performing optimally from an aberration perspective.

The LSI module consists of a 2-dimensional diffraction grating mounted to a 6-axis hexapod for linear and angular positioning. The grating is located at the image conjugate plane of the MET5 optic, which sits at a  $1.12^\circ$  angle from the plane normal to the optical axis. This condition is necessary to ensure that multiplexed sources from the mask create interferograms that all have the same fringe density. The grating assembly is mounted above a water-cooled, 1”-format, in-vacuum CCD from Princeton Instruments used for capturing the interferometry data. The CCD is mounted so that its sensor is parallel to the grating, a condition that was found to minimize systematic aberrations in the system. A schematic of the module geometry is shown in Figure 2.

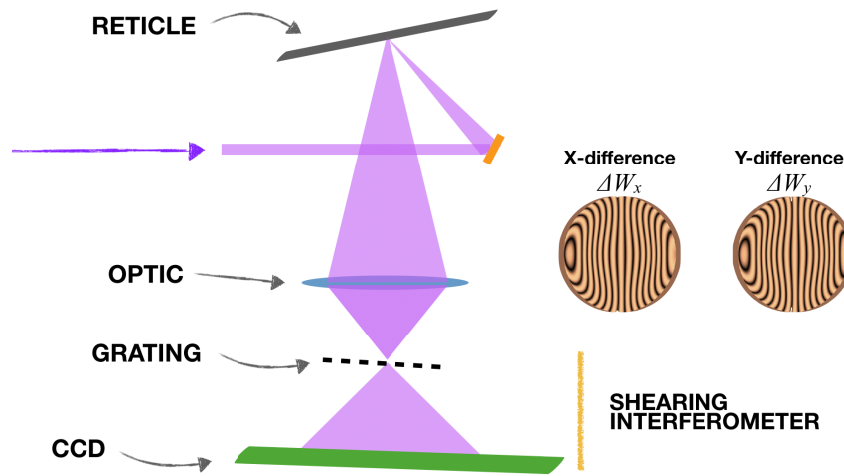


Figure 2. Schematic of the shearing interferometer. The diffraction grating splits the beam into multiple orders onto the detector creating interference patterns along the axes of the grating.

## 2.2 Data collection

The basic details of how a typical grating-based lateral shearing interferometer is used to reconstruct a wavefront can be found elsewhere [3], but broadly, the intensity at the detector is formed from the interference between the test wavefront and laterally shifted copies of itself arising from the grating diffraction orders. The interference fringes therefore contain information related to the wavefront difference functions  $\Delta W_x = W(x, y) - W(x-s, y)$  and  $\Delta W_y = W(x, y) - W(x, y-s)$  along the grating axes.

During the measurement, the CCD records  $N^2$  images as the grating is scanned in  $x$  and  $y$  on an  $N$  by  $N$  grid where each step is  $1/N$  of the grating period (here,  $N$  is typically between 6 and 10). The result is a 2D stack of interferograms with phase shifts in  $x$  and  $y$  at the values  $[0, 2\pi/N, 4\pi/N, \dots, 2\pi - 2\pi/N]$ . Typical phase shifting approaches can be used to compute the wavefront differences  $\Delta W_x$  and  $\Delta W_y$  in the  $x$ - and  $y$ -directions respectively [4]. The final wavefront is reconstructed from its difference wavefronts using a least-squares approach, discussed in section 3.1.

## 2.3 System stability and error correction

A typical data series requires about 5 minutes to collect. During this time, it is important that either the system remain stable to drift caused by thermal fluctuations, or that this drift is monitored and either corrected in real time or compensated in the reconstruction. The most critical axis for drift is the  $z$ , or longitudinal axis, as drift in this direction adds a varying defocus to the interferograms which cannot be easily compensated in the analysis. Because of this, we track the  $z$ -position of the grating using a height sensor [2], and compensate any deviations in real-time at the reticle to ensure that the conjugate condition is preserved. Since the MET5 operates at a 5X demagnification, correcting longitudinal drift at the reticle as opposed to the grating requires 25 times more motion, which significantly relaxes the tolerance on the stage motion.

Drift in the transverse directions can be more readily corrected numerically in the reconstruction. Differential laser interferometers installed in the MET5 chamber track the position of the reticle and grating with respect to the optic and are logged with each image. These positions are then used to create a non-uniform sampling grid over which the phase modulation is fit. This technique relaxes the accuracy requirements on the stage as it performs the grating scan since stage position errors couple into this same correction mechanism.

## 2.4 Multiplexed source and illumination design

One of the key challenges with designing a shearing interferometer for a tool with single-nanometer optical resolution is creating a spherical wave input to the system. A high-quality spherical input is necessary for characterizing the optical system because aberrations in the optic cannot be decoupled from aberrations in the input wave. A standard way of producing a spherical reference is via diffraction through a small pinhole where the pinhole diameter  $D$  is chosen to match the object-side resolution limit of the system. For systems with resolutions of 50 nm and smaller, this is not a practical solution due to the poor efficiency of small pinholes creating insufficient signal in the interferogram.

One accepted solution to this problem is to use pinhole multiplexing [5]. In this setup, multiple pinholes are arrayed in the object plane and each serve as an independent input source to the interferometer. The geometry of the pinhole array must satisfy three criteria:

1. The smallest separation between adjacent pinholes must be large compared with the coherence function width  $w_c$  at the object so that the contribution of each pinhole adds in intensity (incoherently) at the detector.
2. The pinhole spacing must be periodic, and the period  $T_p$  must be an integer multiple of the shearing interferometry grating period  $T_g$  times the magnification  $m$  of the system:  $T_p = nmT_g$ ,  $n \in \mathbb{N}$ . Pinholes that lie outside of this grid contribute phase-shifted interferograms which serve to reduce rather than enhance contrast in the interferogram.
3. The diffraction NA of the pinholes plus the illumination NA must be greater than or equal to the object-side NA of the optical system to ensure that the optic receives light across its entire pupil.

An ostensible solution to satisfy these three requirements would be to use a full disk illumination. Since this illumination fills the pupil NA and the corresponding coherence function at the object is a delta function, criteria 1 and 3 are satisfied by default, and criterion 2 is easily satisfied by setting  $T_p = mT_g$ . The issue is that DC flare coming from light transmitted through the mask absorber causes an image of the pupil fill to be superposed onto the interferograms, and if this fill is not sufficiently uniform, it causes noise in the data.

To overcome this obstacle, a disk illumination of  $0.3\text{-}\sigma$  is employed, as this number matches the angular cutoff of the central obscuration of the Schwartzchild objective. As a result, all of the DC flare is directed into and blocked by the obscuration. To satisfy criterion 3, the pinhole diameter is chosen to be 80 nm, which provides sufficient diffraction to fill the rest of the pupil. In this configuration, criteria 1 and 2 are satisfied by setting  $T_p = mT_g$ , since the coherence width for the illumination is  $w_c = 240$  nm, which is far less than the mask-side grating period of 1.17  $\mu\text{m}$ .

## 2.5 Grating design

The 2D diffraction grating used in the MET5 shearing interferometer was manufactured by the CXRO nanofabrication lab using an 80-nm nickel absorber on top of a 100-nm silicon nitride membrane window. The grating pattern is designed as rotated checkerboard pattern with pitch  $T = 234$  nm generating a shear of 5% across the pupil. Figure 3 contrasts the ideal thin-mask checkerboard grating spectrum to that of a conventional 2D square grating design.

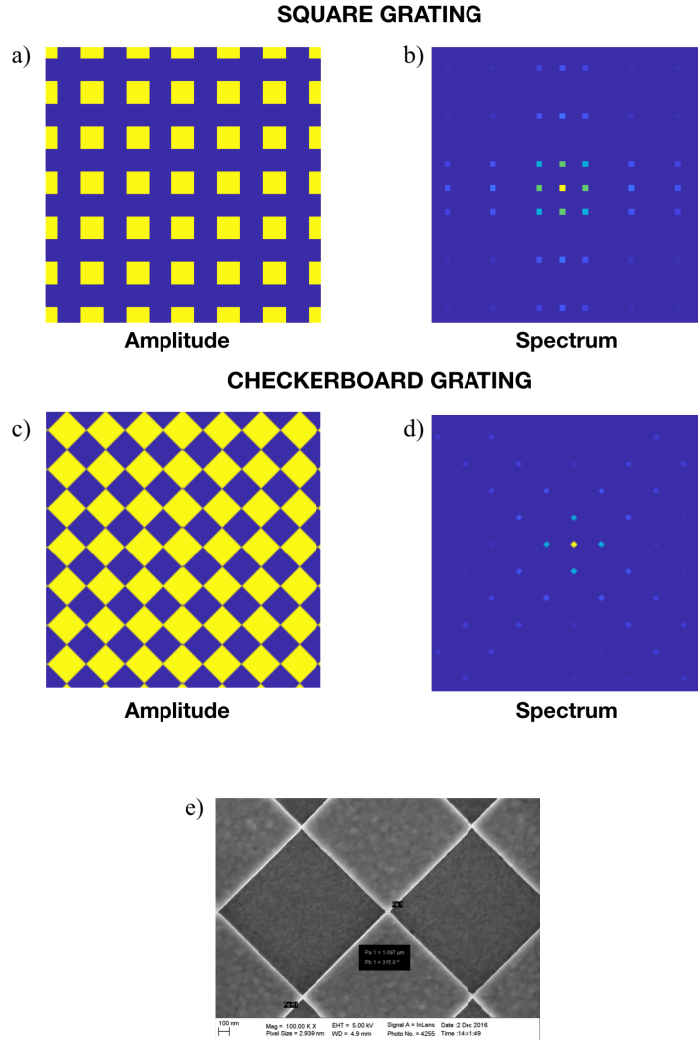


Figure 3. Amplitude and ideal thin-mask spectrum of a 2D square grating (a-b) and a checkerboard grating (c-d). (e) shows SEM image of checkerboard grating manufactured by CXRO

Unlike the square grating, the checkerboard grating has a spectrum where there are only 2 pairs of adjacent orders in  $x$  and  $y$  directions that are separated by the fundamental frequency (in an ideal thin mask). This property allows the resulting interference pattern to have its  $[0, +1]$  and  $[0, -1]$  interference terms isolated numerically.

At high numerical apertures, 3D effects on the grating cause the grating spectra to deviate from the ideal thin mask shown in Figure 3 causing a nonzero contribution of even diffraction orders. This effect theoretically hinders our ability to completely isolate the relevant interference terms, however rigorous 3D modelling using RCWA demonstrates that in the case of the checkerboard grating this additional error is negligible.

### 3. WAVEFRONT RECONSTRUCTION AND MET5 OPTIC CHARACTERIZATION

#### 3.1 LSI reconstruction

To reconstruct the final wavefront from its wavefront difference functions we use a least squares approach that is configurable based on the optical geometry. Historically, grating-based lateral shearing interferograms are reconstructed with a numerical integration method like the Rimmer method [6]. However, these methods typically rely on two

assumptions. The first is that the shear, or lateral displacement between interfering wavefronts, is fixed across the detector plane. The second is that the functional form of the wavefronts in diffracted orders are equivalent to the zeroth order wavefront apart from a lateral (and angular) shift. Both of these are good assumptions for low-NA optical systems, but they break down at high-NA. The MET5 geometry in particular is additionally problematic because due to the multiplexing requirement, the diffraction grating is tilted at  $1.12^\circ$  with respect to the plane normal to the optical axis, giving an added asymmetric angular distortion to the wavefront in diffracted orders.

The consequence of these assumptions not being met is that the “null wavefront” or the wavefront that is reconstructed when the input is a perfect spherical wave, is non-zero. This null wavefront, if not accounted for, will translate into systematic aberrations in the reconstruction.

A rigorous treatment of how to compute and compensate for the null wavefront is given in [7], but broadly, the reconstruction involves building a numerical model of the optical geometry. This serves two purposes: first, it allows the null wavefront to be fully characterized as a function of NA, grating tilt, and grating defocus, and second, it provides the system response to various aberration inputs. Using this model, we create a basis of vectors representing the system response to Zernike polynomials 1-37 realized as difference wavefronts, plus one basis vector representing the null wavefront. To reconstruct the final wavefront, we simply map the experimentally obtained difference wavefronts onto the generated basis, while the null wavefront is simultaneously subtracted.

### 3.2 MET5 wavefront characterization and optical alignment

In October 2018, the MET5 was characterized using its lateral shearing interferometer to have an RMS wavefront of 0.69 nm at the center of the field. The Zernike decomposition revealed that the wavefront was dominated by primary coma terms in the  $x$  and  $y$  directions, each with magnitude of around 1.2 nm. The signature of these aberrations was apparent in prints of radial gratings under annular illumination showing asymmetric contrast as a function of line angle, which is consistent with modeled aerial images. The presence of higher-order spherical aberration was also present ( $Z_{15}$  and  $Z_{24}$ ), however the modeled effects of these aberrations was negligible, and were not a focus of the initial alignment.

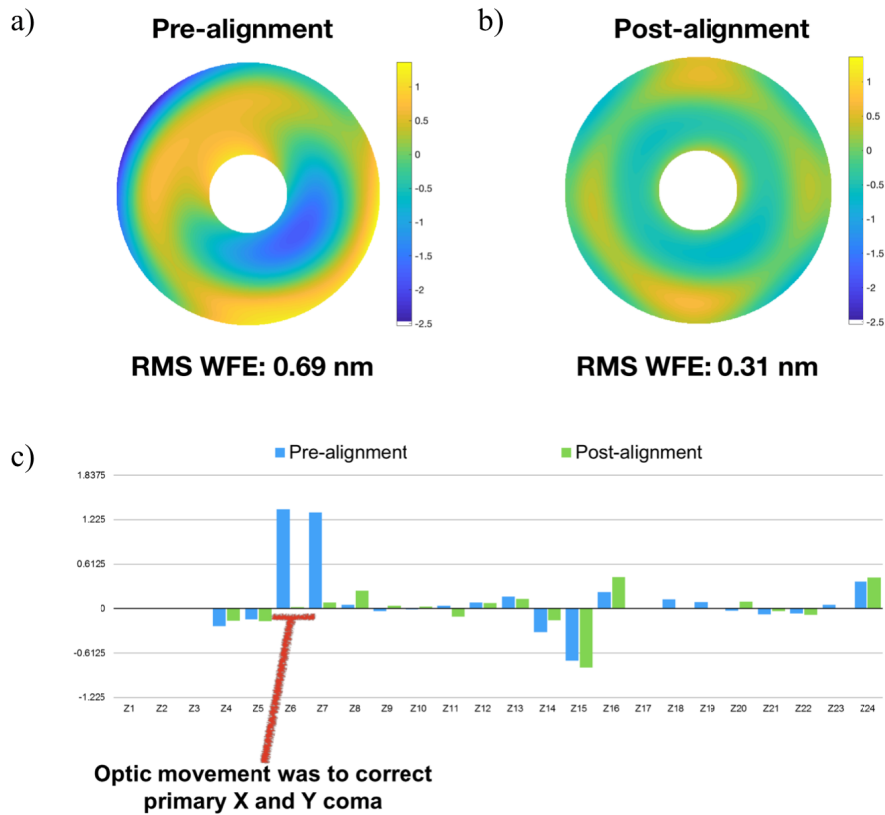


Figure 4. LSI reconstructed aberrations of the MET5 optic before alignment (a) and after alignment (b). (c) shows Zernike decomposition before and after alignment.

The measured aberration signature was fed into an optical model provided by Zygo, which translated this signature into alignment instructions manifesting as small translations and tilts to the MET5 optic. After making these adjustments the optic was remeasured and the resulting wavefront had improved to 0.31 nm, which met the design specification of 0.50 nm at the center of the field. Figure 4 shows the Zernike decomposition of the wavefront before and after the alignment demonstrating the successful removal of the primary coma terms. Figure 5 shows examples of radial gratings printed before and after the primary coma was aligned. Pre-alignment, the aberration signature manifests as an anisotropic contrast with respect to line angle, whereas post-alignment, contrast is high in all line orientations.

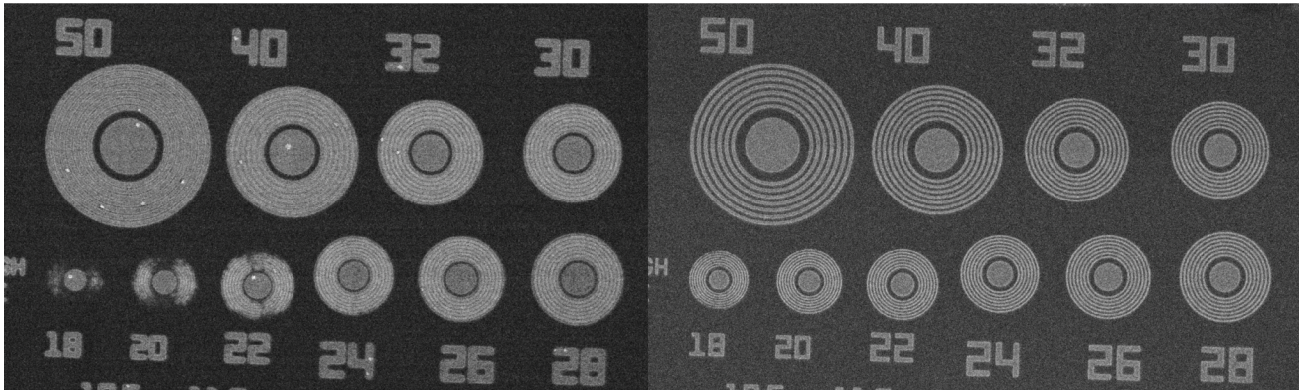


Figure 5. Wafer prints of radial gratings before (left) and after (right) alignment of the primary coma terms

#### 4. DISCUSSION

The integrated shearing interferometry module is a key operating component of the Berkeley MET5 platform, as it provides a convenient means for monitoring the optical aberrations and ensuring that the tool is operating near its diffraction limit. Implementing this interferometer required careful consideration of the many challenges associated with high-NA interferometry including the compensation of drift during the experiment, achieving adequate photon flux via pinhole multiplexing, and a specialized reconstruction that is specific to the geometry of the optical system. Overcoming these challenges has produced a working wavefront sensor suitable for measuring aberrations in optics with NA of 0.5 and greater. While the Berkeley MET5 is a specific application, this technique is readily applicable to other EUV lithography, inspection, and review tools.

This work was performed at Lawrence Berkeley National Laboratory with support from Intel, Samsung, EUV Tech, Inpria, and JSR through the U.S. Department of Energy under Contract No. DE-AC02-05CH11231. Support for the projection optics was also provided by the Department of Energy, Advanced Manufacturing Office.

#### REFERENCES

- [1] Van Schoot, et al. "EUV lithography scanner for sub-8nm resolution." SPIE Advanced Lithography. International Society for Optics and Photonics, (2015).
- [2] Miyakawa, R., et al. "High-NA metrology and sensing on Berkeley MET5" SPIE Advanced Lithography. International Society for Optics and Photonics, (2017).
- [3] Bon, P., et. al. "Quadriwave lateral shearing interferometry for quantitative phase microscopy of living cells" *Op. Ex.* **17**, 15 (2009)

- [4] Creath, K. and Schmit, J. "N-point spatial phase-measurement techniques for non-destructive testing" *Optics and Laers in Engineering*, **24**, 5-6 (1996)
- [5] Ichikawa, Y. et al." High-Precision Wavefront Metrology Using Low Brightness EUV Source", EUVL symposium (2010)
- [6] M. P. Rimmer, "Method for Evaluating Lateral Shearing Interferograms" *Applied Optics* **13**, 3 (1974)
- [7] Zhu, W. et al, "Lateral Shearing Interferometry for high-NA EUV optical testing", *Proc. SPIE 10809*, (2018)